The Plant Journal (2007) **52**, 1154–1168 doi: 10.1111/j.1365-313X.2007.03307.x

Comparison of five xylan synthesis mutants reveals new insight into the mechanisms of xylan synthesis

David M. Brown[1,†], Florence Goubet[2,†,‡], Vicky W. Wong[2,§], Royston Goodacre[3], Elaine Stephens[4], Paul Dupree[2] and Simon R. Turner[1,*]

[1]*Faculty of Life Science, University of Manchester, Manchester M13 9PT, UK,*
[2]*Biochemistry Department, Building O, Downing Site, Cambridge CB2 1QW, UK,*
[3]*School of Chemistry and Manchester Interdisciplinary Biocentre, University of Manchester, Manchester M13 9PT, UK, and*
[4]*Chemistry Department, University of Cambridge, Lensfield Road, Cambridge, CB2 1EW, UK*

Received 4 July 2007; accepted 23 August 2007.
[*]For correspondence (fax +44 161 2753938; e-mail simon.turner@manchester.ac.uk).
[†]These authors contributed equally to this paper.
[‡]Present address: Bayer BioScience N.V., Technologiepark 38, B-9052 Zwijnaarde, Belgium.
[§]Present address: McGill Cancer Centre, McGill University, Montreal, Quebec, H3G 1Y6, Canada.

Summary

Previous studies using co-expression analysis have identified a large number of genes likely to be involved in secondary cell-wall formation. However, the function of very few of these genes is known. We have studied the cell-wall phenotype of *irx7*, *irx8* and *irx9*, three previously described *irregular xylem* (*irx*) mutants, and *irx14* and *parvus-3*, which we now show also to be secondary cell-wall mutants. All five mutants, which have mutations in genes encoding putative glycosyltransferases, exhibited large decreases in xylan. In addition, all five mutants were found to have the same specific defect in xylan structure, retaining MeGlcUA but lacking GlcUA side branches. Polysaccharide analysis by carbohydrate gel electrophoresis (PACE) was used to determine the xylan structure in Arabidopsis, and revealed that side branches are added to approximately one in every eight xylose residues. Interestingly, this ratio is constant in all the lines analysed despite the wide variation in xylan content and the absence of GlcUA branches. Xylanase digestion of xylan from wild-type plants released a short oligosaccharide sequence at the reducing end of the xylan chain. MALDI-TOF MS analysis indicated that this sequence of sugars was absent in xylan from *irx7*, *irx8* and *parvus-3* mutants, but was present in *irx9* and *irx14*. This is consistent with previous NMR analysis of xylan from *irx7*, *irx8* and *irx9*, and suggests that PARVUS may be involved in the synthesis of a xylan primer whereas IRX14 may be required to synthesize the xylan backbone. This hypothesis is supported by assays showing that *irx9* and *irx14* are both defective in incorporation of radiolabel from UDP ^{14}C-xylose. This study has important implications for both our understanding of xylan biosynthesis and the functional analysis of cell-wall biosynthesis genes.

Keywords: xylan, glycosyltransferase, secondary cell wall, glucuronic acid, *irregular xylem* (*irx*) mutant.

Introduction

The importance of understanding xylan synthesis is highlighted by the increasing significance of plant biomass as a potential source of renewable energy. Decreases in non-renewable energy resources have led to a projected increase in the production of bio-fuels (Ragauskas *et al.*, 2006). It has been proposed that the woody tissues of plants (composed predominantly from cellulose, xylan and lignins) can be used as a source of bio-fuel (Bevan and Franssen, 2006). One of the obstacles to manipulating plant cell walls for more efficient utilization is the problem associated with identifying the enzymes that catalyse individual steps in secondary cell-wall formation. More than 800 putative glycosyltransferases and glycosyl hydrolases have been identified in Arabidopsis, and many of these are likely to be involved in some aspect of cell-wall formation.

Xylans are the major constituent of hemicellulose in the secondary cell walls of dicotyledonous plants, and, as a major constituent of wood, are one of the most abundant

biopolymers on earth. Consequently, the elucidation of xylan metabolism will not only answer important biological questions, but may also have implications for the emerging bio-renewable energy industry and other wood-dependent industries.

Xylans are polysaccharides composed from a backbone of β(1,4)-linked xylose (Xyl) sugars (Ebringerova and Heinze, 2000). They may also contain arabinose (Ara), glucuronic acid (GlcUA) and 4-*O*-methyl glucuronic acid (Me-GlcUA) side branches (Ebringerova and Heinze, 2000). In addition, a complex oligosaccharide sequence [β-D-Xyl-(1,4)-β-D-Xyl-(1,3)-α-L-Rha-(1,2)-α-D-GalUA-(1,4)-D-Xyl] has been found on the reducing ends of xylan chains, and appears to be highly conserved in a number of divergent species (Andersson and Samuelson, 1983; Johansson and Samuelson, 1977; Peña *et al.*, 2007). Although structurally very well characterized, much less is known about the enzymes that synthesize xylan or the genes that encode these enzymes.

Transcriptomic studies based on the co-variance of secondary cell-wall-specific cellulose synthase genes have identified a number of Arabidopsis genes that are essential for correct secondary cell-wall formation (Brown *et al.*, 2005; Persson *et al.*, 2005). T-DNA insertion mutants corresponding to three of these genes (termed *irx7*, *irx8* and *irx9*) show large reductions in Xyl in the inflorescence stem (Brown *et al.*, 2005). Furthermore, Fourier-transform infra-red (FTIR) spectroscopy with chemometric analysis indicates that the alteration in cell-wall composition associated with these mutants is consistent with a lack of β(1-4)-linked xylosyl residues associated with xylan (Brown *et al.*, 2005). Cell-wall fractionation and immunolabelling have demonstrated a specific reduction in Xyl in the major xylan-containing fractions of the cell wall (Peña *et al.*, 2007; Persson *et al.*, 2007; Zhong *et al.*, 2005). Characterization of *fra8*, which is allelic to *irx7*, indicates a lack of GlcUA side branches but retention of side branches containing Me-GlcUA (Zhong *et al.*, 2005). Recent studies have shown that *irx8* and *irx9* also exhibit this defect (Peña *et al.*, 2007; Persson *et al.*, 2007), and additionally that *irx7* and *irx8* lack the complex oligosaccharide sequence normally found at the reducing ends of xylan. Furthermore, although *irx9* was found to possess this complex oligosaccharide, xylan chain length was greatly reduced compared to wild-type, indicating a defect in xylan chain elongation (Peña *et al.*, 2007). These differences suggest a separate role for IRX7 and IRX8 in synthesis of the reducing end oligosaccharide, while IRX9 may be involved in chain elongation (Peña *et al.*, 2007).

Plant glycosyltransferases have been classified into sequence-related families that reflect similarities in their mechanism of action (Coutinho *et al.*, 2003). IRX7, IRX8 and IRX9 are members of glycosyltransferase (GT) families 47, 8 and 43 respectively. Whilst members of GT family 8 are thought to catalyse the formation of α-glycosidic bonds using α-linked donor substrates, GT43 and GT47 families comprise members that have inverting enzyme activity (Coutinho and Henrissat, 1999).

This study describes the identification of two further Xyl-deficient mutants, *irx14* and *parvus*. Detailed analysis of these novel mutants showed that they exhibit a specific and dramatic reduction in xylan similar to that in the previously described xylan-deficient mutants *irx7*, *irx8* and *irx9*. *irx14* and *parvus-3* also share the same large decrease in the ratio of GlcUA to Me-GlcUA side chains observed in *irx7*, *irx8* and *irx9*. Absence of the complex oligosaccharide suggests that xylan biosynthesis in *parvus-3* is defective in a manner similar to that in *irx7* and *irx8*, whereas this structure is present in *irx14*. Analysis of xylosyltransferase activity is consistent with a role for *PARVUS* together with *IRX7* and *IRX8* in the synthesis of a primer, with *IRX9* and *IRX14* being involved in elongation of the xylan backbone. The novel application of polysaccharide analysis by carbohydrate gel electrophoresis (PACE) to the Arabidopsis xylan structure showed that a side branch is added to one in eight Xyl resides. This ratio remains constant in all the mutants despite the large differences in the amount of xylan and the absence of one of the GlcUA side branches, suggesting that a remarkably robust mechanism regulates the addition of side branches to the xylan backbone. The data demonstrate a requirement for both *IRX14* and *PARVUS* in normal xylan biosynthesis.

Results

Identification of additional putative glycosyltransferases expressed during secondary cell-wall deposition

Previous studies have demonstrated that the level of secondary cell-wall metabolism varies considerably in the inflorescence stem, leaf and hypocotyl. This variance is mirrored by large changes in gene expression, allowing genes involved in secondary cell-wall metabolism to be identified on the basis of co-variance in expression with known secondary cell-wall genes such as *IRX3* (Brown *et al.*, 2005; Persson *et al.*, 2005). This gene encodes a GT2 protein that is essential for normal cellulose synthesis during secondary cell-wall formation (Taylor *et al.*, 2003; Turner and Somerville, 1997).

To extend the previous study by Brown *et al.* (2005), a similar analysis was performed on a larger dataset derived by combining existing data with publicly accessible microarray experiments available through NASC (http://affymetrix.arabidopsis.info) (data not shown). Using this enlarged dataset, with previously described methods (Brown *et al.*, 2005), two further genes encoding putative glycosyltransferases were identified that exhibited good gene expression co-variance with *IRX3*. The genes At1g19300 and At4g36890 are members of the GT8 and GT43 families, respectively. Linear regression analysis of At1g19300 and At4g36890

expression against *IRX3* using a large number of publicly available datasets at the Genevestigator site (Zimmermann *et al.*, 2004) indicated that both had r^2 values of 0.68. In addition to their clear expression correlation with *IRX3*, other evidence indicates that these genes are required for secondary cell-wall synthesis. Previous work has identified two mutants, *parvus* and *gaolaozhuangren1* (*glz1*), caused by alterations in At1g19300 (Lao *et al.*, 2003; Shao *et al.*, 2004). Promoter–GUS fusion studies on At1g19300 have shown that this gene is predominantly expressed in areas of high secondary cell-wall synthesis, such as the vascular tissue (Shao *et al.*, 2004). Furthermore, transcriptomic analyses have demonstrated that expression of the poplar homologue of *PARVUS/GLZ1*, PttGT8E/F, was highly upregulated in tissues undergoing secondary cell-wall formation (Aspeborg *et al.*, 2005; Prassinos *et al.*, 2005). *parvus/glz1* plants are also generally smaller and darker green compared to wild-type, a phenotype that is reminiscent of several secondary cell-wall mutants (Brown *et al.*, 2005).

At4g36890 is a member of GT family 43. This family has only four members in Arabidopsis, one of which (*IRX9*) has already been shown to be required for normal secondary cell-wall synthesis (Brown *et al.*, 2005). Considering this evidence, At1g19300 and At4g36890 were regarded as good candidate genes required for secondary cell-wall synthesis.

Characterization of T-DNA insertion mutants

T-DNA insertion lines were selected using the SIGnAL database (http://signal.salk.edu/). We obtained T-DNA insertions for both At1g19300 (SALK_045368) and At4g36890 (SALK_038212), positioned in the 5′ UTR and exon, respectively. In order to verify the effect of the insertions on mRNA expression, RT-PCR was performed using gene-specific primers. The primer pairs generated a PCR fragment of the predicted size in the wild-type that was almost undetectable in the SALK_038212 insertion line and greatly reduced in the SALK_045368 insertion line (Figure S1A).

Xylem morphology was determined by cutting sections from the base of the mature inflorescence stem. Both insertion lines exhibited a clear irregular xylem phenotype that was similar in severity to that of *irx8* (Figure 1) and other *irx* mutants such as *irx7* and *irx9* (Brown *et al.*, 2005). As the insertion line corresponding to At4g36890 has not previously been described, it was designated *irx14*. Transformation of *irx14* with the wild-type version of At4g36890 resulted in restoration of the xylem phenotype, thus unambiguously demonstrating that the defect was caused by a mutation in this gene (Figure S1B). A mutation in At1g19300 has already been described by two independent studies and named *parvus* (Lao *et al.*, 2003) and *glz1* (Shao *et al.*, 2004). Consequently, this third mutant allele will be referred to as *parvus-3*.

The whole-plant morphologies of *irx14* and *parvus-3* are shown in Figure 1. The overall development of *irx14* was comparable to that of the wild-type, and only small differences in gross morphology were observed. On average, stems were thinner and shorter, and had less well-developed siliques and fewer seeds. *parvus-3* plants developed in a similar manner to the previously identified *irx* mutants, *irx7*, *irx8* and *irx9*. They developed more slowly, were dark green, had narrower leaves and were almost completely sterile. The plant morphology of *parvus-3* was characteristic of the previously studied alleles *parvus* and *glz1* (Lao *et al.*, 2003; Shao *et al.*, 2004).

Cell-wall composition

The sugar composition of the non-cellulose carbohydrate fraction of the stems of *irx14* and *parvus-3*, along with those of *irx7*, *irx8* and *irx 9*, was determined by measurement of alditol acetates using gas chromatography (GC) (Figure 2a). The results are in general agreement with those of previous studies (Brown *et al.*, 2005; Turner and Somerville, 1997), with Xyl being the major neutral sugar in wild-type stems. Also consistent with prior analysis is the large decrease in Xyl in *irx7*, *irx8* and *irx9* (Brown *et al.*, 2005; Zhong *et al.*, 2005). A similar decrease (<50% of wild-type levels) was also

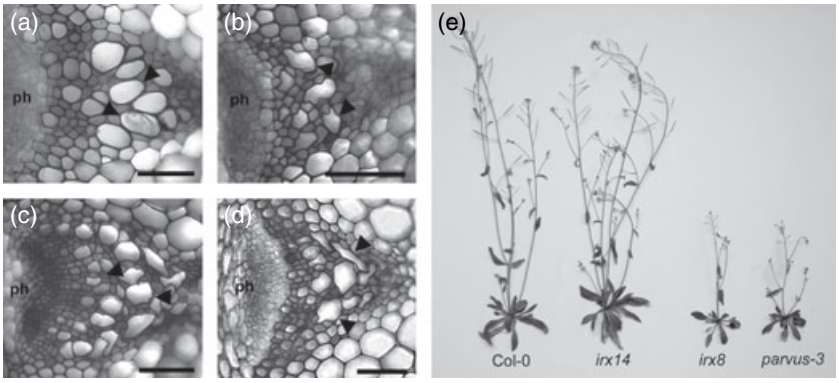

Figure 1. Vascular bundle and whole-plant morphology of wild-type and *irx* mutant plants.
(a–d) Transverse stem sections stained with toluidine blue. A single representative vascular bundle is shown from each mutant. The phloem (ph) and xylem vessels (arrowheads) are indicated. (a) Columbia wild-type, (b) *irx8*, (c) *irx14*, (d) *parvus-3*. Bar = 50 μm.
(e) Whole-plant morphology of wild-type and *irx* mutants. All plants shown were 6 weeks old.

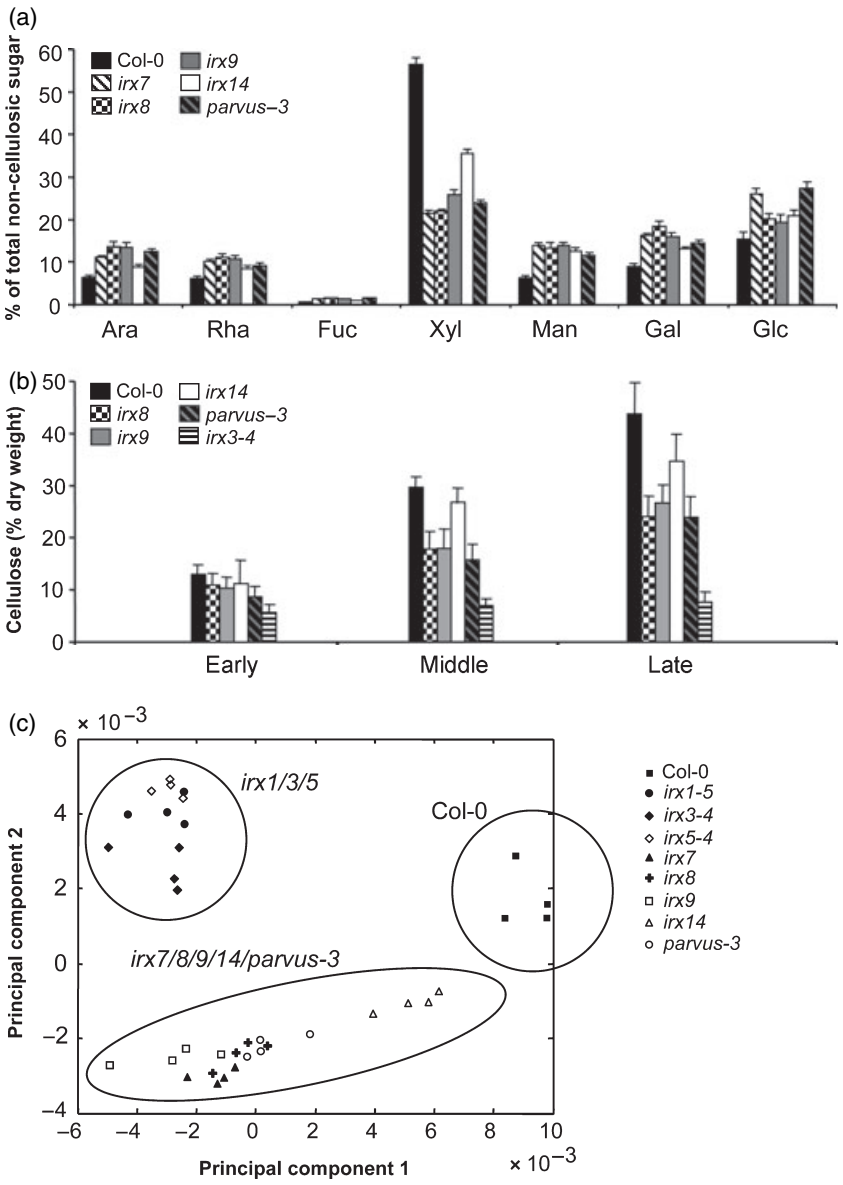

Figure 2. Analysis of cell-wall material from stems of wild-type and *irx* mutant plants.
(a) The non-cellulosic carbohydrate composition of cell-wall material. The individual sugars arabinose (Ara), rhamnose (Rha), fucose (Fuc), xylose (Xyl), mannose (Man), galactose (Gal) and glucose (Glc) are expressed as a percentage of the total recoverable sugar. Standard error bars are shown ($n = 3$).
(b) Cellulose content of developing stems expressed as a proportion of the ethanol-insoluble cell-wall material. Standard error bars are shown ($n = 3$).
(c) PCA of FTIR spectra from wild-type and mutant stem material. PC1 accounted for 58.5% of the total explained variance, whereas PC2 accounted for 22.4%.

observed in the stems of *parvus-3*. *irx14* stems were also found to have a reduction in Xyl, but this was less severe than the decreases observed in *irx7*, *irx8*, *irx9* and *parvus-3* (Figure 2a).

Cellulose content was measured in the stems of the *irx14* and *parvus-3* mutants and in the stems of *irx3-4*, *irx8* and *irx9* for comparison. To overcome the potential problem with measuring the cellulose content of plants with altered morphology (Brown *et al.*, 2005; Turner and Somerville, 1997), all lines were examined at three stages of development (Figure 2b). Wild-type plants exhibited an increase in cellulose content in the stem during development that reflects the increase in secondary cell-wall deposition (Figure 2b). In agreement with previous studies (Brown *et al.*, 2005), *irx3-4* plants did not show an increase in cellulose during stem development, and consequently at late stages of stem development they only have 20% of the cellulose content of the wild-type (Figure 2b). In contrast, *irx14* and *parvus-3* exhibit an obvious increase in cellulose content during development in a manner similar to that in *irx8* and *irx9*. The relative accumulation of cellulose during development is similar to that in wild-type, although at each stage the cellulose content is less than that of corresponding wild-type plants (Figure 2b).

Previous studies have shown FTIR spectroscopy to be an effective means of characterizing and grouping secondary cell-wall mutants (Brown *et al.*, 2005). Consequently FTIR was performed on *irx14* and *parvus-3* as well other known secondary cell-wall mutants *irx1*, *irx3*, *irx5*, *irx7*, *irx8* and *irx9* (Brown *et al.*, 2005; Taylor *et al.*, 2003; Turner and

Somerville, 1997). Principal component analysis (PCA) scores plot derived from FTIR spectra data separated the mutant lines into distinct clusters on the basis of secondary cell-wall defects (Figure 2c). *irx1*, *irx3* and *irx5* and *irx7*, *irx8* and *irx9* separated from wild-type into two clusters. The principal component (PC) loadings were very similar to our previous FTIR analysis (Brown *et al.*, 2005), indicating that separation on PC1 is mainly caused by differences associated with cellulose, whilst separation on PC2 was a result of differences associated with Xyl content (data not shown). *irx14* and *parvus-3* also separated from wild-type, with *parvus-3* grouping closely with *irx7*, *irx8* and *irx9*, and *irx14* forming a single cluster close by (Figure 2c). The grouping of *parvus-3* in the same region of the plot as *irx7*, *irx8* and *irx9* suggests a common cell-wall defect (Figure 2c). Furthermore, these data agree with cellulose and cell-wall sugar measurements and indicate that *irx14* shows a similar, but somewhat weaker, phenotype compared to *irx7*, *irx8*, *irx9* and *parvus-3* (Figure 2).

Fractionation of cell-wall polysaccharides

Chemical separation of the cell wall was performed to isolate xylan-containing fractions. Cell walls derived from the inflorescence stem were sequentially extracted in 1,2-cyclohexanediaminetetraacetic acid (CDTA), Na_2CO_3, 1 M KOH and 4 M KOH. The resultant determination of neutral sugars and uronic acids is shown in Figure 3.

The largest alterations were found in the 1 M KOH fraction. This procedure solubilizes significant amounts of acidic xylan in addition to residual pectins by disrupting the hydrogen bonding between the xylans and the cellulosic microfibrils (Coimbra *et al.*, 1996). Consistent with this, the wild-type 1 M KOH fraction consisted of 75% Xyl, 5% Me-GlcUA and 2% GlcUA, indicating that xylan is the predominant polysaccharide. The amounts of these monosaccharides appear to increase in *irx3-4*; however, this is likely to result from the absence of cellulose, making xylan a larger proportion per unit mass of the cell wall (Figure 3). In agreement with previous studies (Peña *et al.*, 2007; Persson *et al.*, 2007; Zhong *et al.*, 2005), *irx7*, *irx8* and *irx9* exhibited significant decreases in Xyl (Figure 3). The analysis of *irx14* and *parvus-3* revealed Xyl reductions comparable to those of *irx7*, *irx8* and *irx9.* Levels of GlcUA were also reduced in these mutants. In contrast, the ratio of Me-GlcUA to Xyl increased (Figure 3). Taken together, these results suggest that *irx14* and *parvus-3* have reduced levels of xylan in the inflorescence stem similar to those in *irx7*, *irx8* and *irx9*. They also suggest that the proportions of GlcUA and Me-GlcUA side branches are altered compared to wild-type.

High-concentration alkali extraction of plant cell walls solubilizes predominantly non-acidic hemicelluloses such as glucomannans and xyloglucans, as well as any remaining xylans (Coimbra *et al.*, 1996). Sugar analysis of 4 M KOH cell-wall extractions is shown in Figure 3. The amounts of Xyl detected in the 4 M KOH fraction were reduced in all mutant lines previously shown to have Xyl deficiencies. Also, decreases in GlcUA and increases in Me-GlcUA proportions, relative to Xyl, were observed in these mutant lines. These alterations in cell-wall composition mirror the changes observed in the corresponding 1 M KOH fractions. The reductions in Xyl, however, were smaller in the 4 M KOH fractions compared to the 1 M KOH fractions. This probably reflects the lower proportion of xylan in this fraction. Analysis of the cell-wall residue remaining after alkali extraction found a substantial decrease in Xyl in both *irx9* and *irx14* compared to wild-type (Figure 3). Interestingly, this decrease was not observed to the same extent in *irx7*, *irx8* or *parvus-3*. Glucose, however, was found to dominate the cell-wall residue, and accounted for the majority of the recoverable sugar in all lines analysed except *irx3-4*. It is likely that a large proportion of this glucose is derived from the partial hydrolysis of cellulose.

Other complex changes were also observed within the CDTA and Na_2CO_3 fractions. These fractions contain mainly galacturonic acid (GalUA) (50–60%), with substantial amounts of Ara, rhamnose (Rha) and galactose (Gal), consistent with the extraction of pectic polysaccharides (Figure 3) (Fry, 2000). The total sugars recovered from both the CDTA and Na_2CO_3 fractions for *irx7*, *irx8*, *irx9*, *irx14* and *parvus-3* were all greater than for wild-type (Figure 3), and it appeared that the amount was proportional to the severity of the plant growth phenotype. As this effect was also observed in the cellulose-deficient mutant *irx3-4*, it is likely to be a consequence of alterations in plant development.

PACE of Xyl-deficient mutants

While cell-wall fractionation indicated a decrease in Xyl in the acidic hemicellulose fraction, consistent with a decrease in xylan, other polysaccharides may also contribute to this fraction. To characterize the xylans in the mutants, PACE was performed using β-xylanase digestions of cell-wall material. PACE has been used to study cell-wall polysaccharides quantitatively by exploiting specific cell-wall-degrading enzymes and separating the released oligosaccharides in polyacrylamide gels (Barton *et al.*, 2006; Handford *et al.*, 2003). Here, the technique was adapted by use of a xylanase for the specific analysis of β-(1-4) xylan. Xylan hydrolysis was optimized by de-esterification and extraction from the cell walls using 4 M NaOH. Using this solubilization procedure and treatment with excess pure xylanase from glycosyl hydrolase family 10 (Xyl10A), the enzyme-accessible xylan was essentially completely hydrolysed (data not shown). Use of excess xylanase enzyme also ensured that the xylan was hydrolysed to a few small enzyme-resistant oligosaccharides that could be easily characterized and quantified. Quantification of the released oligosaccharides by PACE

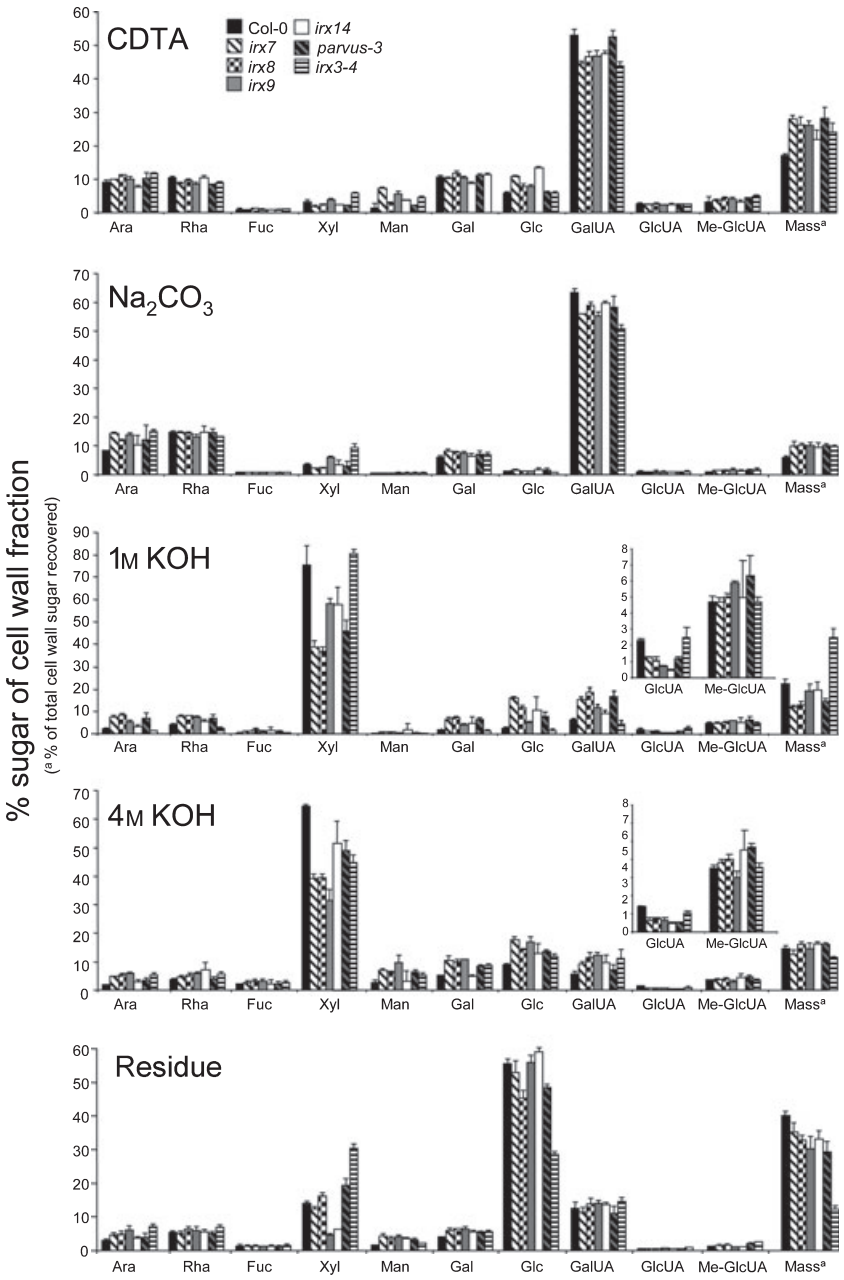

Figure 3. Carbohydrate composition of cell-wall fractions from stems of wild-type and *irx* mutant plants.
Alcohol-insoluble cell wall material was sequentially extracted with CDTA, Na_2CO_3,1 M KOH and 4 M KOH. Individual sugars are expressed as a percentage of the cell-wall fraction. The scale for GlcUA and Me-GlcUA quantities in the 1 M and 4 M KOH fractions has been adjusted to highlight the reductions in GlcUA in the xylose-deficient mutants. Mass indicates the percentage of total wall sugar recovered for a fraction. Standard error bars are shown (n = 3).

showed that this enzyme-accessible xylan represented 9–12% of wild-type stem cell wall samples (data not shown). This is in reasonable agreement with the cell-wall fractionations in which the total quantity of Xyl extracted in the 1 M and 4 M KOH hemicellulose fractions was 8%.

Figure 4(a) shows the β-xylanase PACE of wild-type and *irx* mutants. The fingerprint of hydrolysed wild-type xylan revealed two enzyme-specific bands corresponding to Xyl and $(Xyl)_2$, and a third band containing both $GlcUA(Xyl)_3$ and $Me\text{-}GlcUA(Xyl)_3$, which co-migrated in the gel as they are very similar in mass and structure. The identity of the oligosaccharides in this band was determined by extraction from the gel followed by MALDI-TOF MS/MS (data not shown). Other minor bands were present, but these were considered non-specific background from the enzyme as they were visible in the absence of the cell-wall substrate (Figure S2), and were excluded from the analysis. There was no evidence for oligosaccharides with arabinose substitution, and no bands corresponding to partly digested xylan were detected.

The PACE fingerprints for all the mutants were very similar to those for wild-type, but the intensity of the bands varied (Figure 4a). With the exception of *irx3-4*, all mutants had reduced band intensities compared to wild-type. The amount of the three xylan-derived bands – Xyl, $(Xyl)_2$ and $[Me\text{-}]GlcUA(Xyl)_3$ – was used to measure total enzyme-accessible xylan (Table 1). *irx7* showed the largest decrease

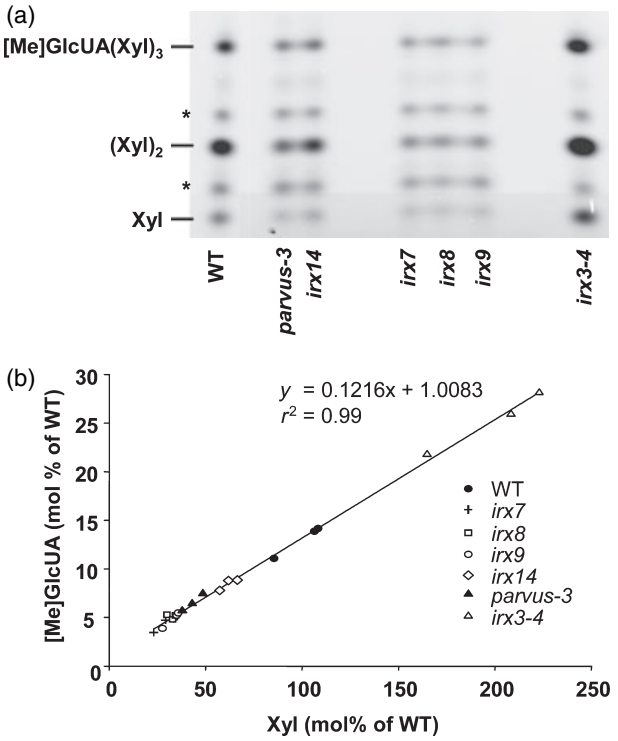

Figure 4. Xylan analysis of *irx* mutants by PACE.
Oligosaccharides, released from alcohol-insoluble cell-wall material digested with xylanase to completion, were derivatized with ANTS (8-aminonaphthalene-1,3,6-trisulfonic acid) and separated by polyacrylamide gel electrophoresis.
(a) Three main oligosaccharide bands were seen: xylose, $(Xyl)_2$ and one band containing both Me-GlcUA$(Xyl)_3$ and GlcUA$(Xyl)_3$ ([Me]-GlcUA$(Xyl)_3$). The other bands, marked with asterisks, are non-specific products from the enzyme or cell-wall preparation.
(b) Measurement of [Me]-GlcUA side branching. Side branching was determined from the quantity of GlcUA in [Me-]GlcUA$(Xyl)_3$ relative to xylose in Xyl, $(Xyl)_2$ and [Me-]GlcUA$(Xyl)_3$. Values are expressed relative to the quantity of xylose backbone in wild-type and are derived from three independent xylanase digests of the wall. These results are consistent with those of an independent biological replicate.

in xylan, with only 29% of wild-type, while *irx14* showed the smallest decrease (57% of wild-type). The reduction in band intensity generally mirrored the decreases of Xyl found in the 1 M KOH fractions of these lines, and demonstrates that *irx7*, *irx8*, *irx9*, *irx14* and *parvus-3* are xylan-deficient mutants. In contrast to the other mutants, *irx3-4* exhibited an approximately 50% increase in xylan per unit of cell-wall material compared to wild-type, probably reflecting the greater proportion of non-cellulosic sugars in these walls. Using PACE, the percentage of Xyl substituted by either GlcUA or Me-GlcUA can be determined from the relative quantities of the Xyl, $(Xyl)_2$ and [Me-]GlcUA$(Xyl)_3$ oligosaccharide bands. The substitution was found to be constant in all lines analysed. The gradient of the relative quantities of Xyl, $(Xyl)_2$ and [Me-]GlcUA$(Xyl)_3$ in each line compared to wild-type was calculated as 0.12 (r^2 = 0.99) (Figure 4b). This gives a ratio of approximately 8:1 for Xyl:[Me-]GlcUA

Table 1 Xylan quantity in stems of wild-type and *irx* mutant plants determined by PACE

Genotype	Percentage xylan/WT
WT	100
irx7	29.2 ± 5.8
irx8	38.8 ± 11.3
irx9	38.3 ± 11.9
irx14	57.0 ± 8.6
parvus-3	45.4 ± 3.9
irx3-4	155.7 ± 16.6

Oligosaccharides released by xylanase from cell-wall material were quantified using PACE, and the total enzyme-accessible xylan quantity is expressed relative to levels from wild-type plant cell walls. Xylose, $(Xyl)_2$ and [Me]-GlcUA$(Xyl)_3$ were quantified. Values are means ± SD of measurements from three xylanase digests analysed in at least 15 gels. The results are consistent with those of a second independent experiment.

(Figure 4b). This result indicates that the frequency of side branches on the xylan backbone remains constant in these mutants despite the large variation in the amount of xylan.

Mass spectrometry analysis of xylans

The monosaccharide analysis suggested that the relative proportions of GlcUA and Me-GlcUA side branches are altered in *irx14* and *parvus-3*, similar to the defect observed in *irx7*, *irx8* and *irx9* (Peña *et al.*, 2007; Zhong *et al.*, 2005). To study this in more detail, the oligosaccharides obtained by hydrolysis of the cell-wall material with Xyl10A were studied by MALDI-TOF MS. The oligosaccharides were first per-deuteromethylated to ensure that the GlcUA$(Xyl)_3$ and Me-GlcUA$(Xyl)_3$ oligosaccharides would ionize with similar efficiency, and also to improve the quality of the spectra. MS analysis revealed that GlcUA$(Xyl)_3$ (*m/z* 800 $[M + Na]^+$) and Me-GlcUA$(Xyl)_3$ (*m/z* 797 $[M + Na]^+$) were both detectable in samples from the wild-type cell walls (Figure 5). Larger [Me]-GlcUA$(Xyl)_n$ oligosaccharides were not detected, confirming that all the substituted regions of the xylan were digested by Xyl10A to this single oligosaccharide. The MS spectrum from *irx3-4* cell walls was very similar to that of wild-type (Figure S3). In contrast, the relative proportion of GlcUA$(Xyl)_3$ to Me-GlcUA$(Xyl)_3$ was substantially reduced in all the other mutants (Figures 5 and S3). It has previously been observed that GlcUA was undetectable in xylan of *fra8* (Zhong *et al.*, 2005; allelic to *irx7*), and recently also in *irx8* and *irx9* (Peña *et al.*, 2007; Persson *et al.*, 2007; Zhong *et al.*, 2005). The results presented here confirm these studies and also indicate that these alterations to xylan structure are common to *irx14* and *parvus-3*.

Xylan of Arabidopsis contains a complex oligosaccharide sequence at the reducing end of the chain. This oligosaccharide, identified by NMR as β-D-Xyl-(1,4)-β-D-Xyl-(1,3)-α-L-Rha-(1,2)-α-D-GalUA-(1,4)-D-Xyl, was found to be absent in

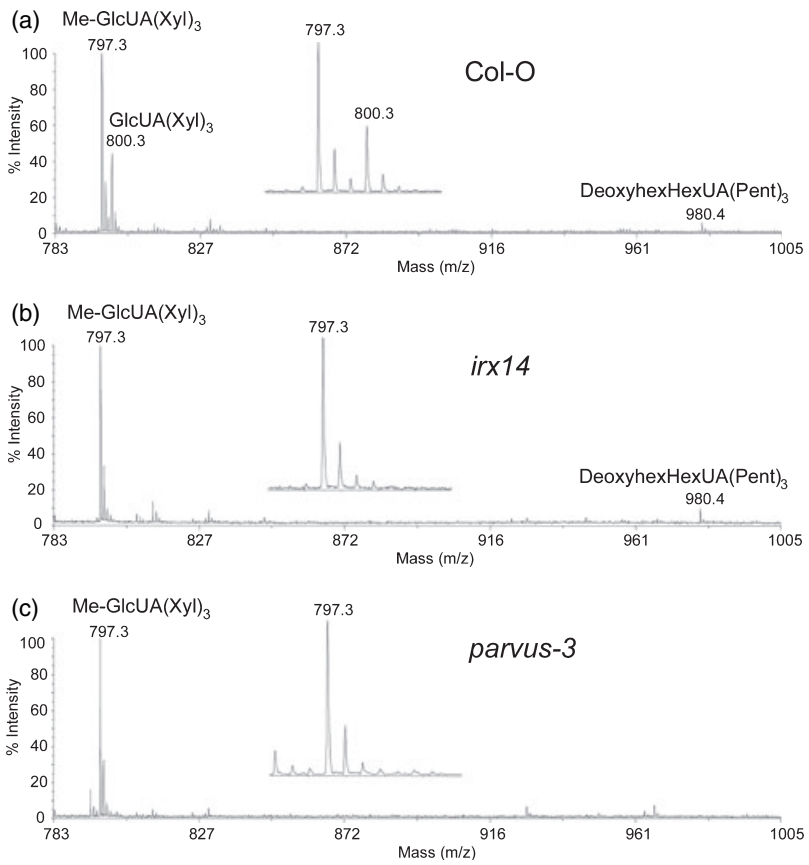

Figure 5. MALDI-TOF MS spectra showing signals for the perdeuteromethylated [Me]-GlcUA(Xyl)$_3$ oligosaccharides produced by xylanase digestion of cell-wall xylan.
The signals at *m/z* 797 [M + Na]$^+$ and *m/z* 800 [M + Na]$^+$ correspond to Me-GlcUA(Xyl)$_3$ and GlcUA(Xyl)$_3$, respectively, and are shown enlarged in the insets. The signal at *m/z* 980 [M + Na]$^+$ corresponds to the reducing-end oligosaccharide.
(a) Wild-type, (b) *irx14*, (c) *parvus-3*.

irx7 and *irx8* but present in *irx9* (Peña *et al.*, 2007). The MS spectrum of xylanase-digested wild-type cell walls revealed a minor signal at *m/z* 980 (Figure 5), which corresponded to this reducing-end oligosaccharide. Subsequent structural analysis by MALDI-TOF/TOF tandem MS produced a series of Y_n and $^{1,5}X_n$ fragment ions (Domon and Costello, 1988) that confirmed the sequence to be pentose–pentose–deoxyhexose–hexuronic acid–pentose (Figure 6). Other ions in the MALDI-MS/MS spectrum (e.g. E_n, D_n G_n) indicate branching and linkage positions (Maslen *et al.*, 2007; Spina *et al.*, 2004), and are also consistent with the reported reducing-end structure. Reduction of the cell-wall polysaccharides with $NaBH_4$ prior to xylanase digestion resulted in a shift in mass of this oligosaccharide to *m/z* 999 [M + Na]$^+$, confirming that it is present at the reducing end of the chain (Figure S4). The oligosaccharide was also found in xylanase digests of cell walls from *irx9*, *irx14* and *irx3-4* (Figures 5 and S3). However, it was absent in similar MS analyses of *irx7*, *irx8* and *parvus-3*, indicating that the reducing end is altered in these three mutants.

Xylosyltransferase activity of the xylan-deficient mutants

Assays were performed to investigate any differences in xylan xylosyltransferase activity in the wild-type and mutant lines. Previous studies in barley (*Hordeum vulgare* L.) and wheat (*Triticum aestivum* L.) indicated that incorporation of Xyl from UDP-Xyl by β(1,4)-xylosyltransferases increased markedly in the presence of exogenous β(1,4)-xylooligosaccharide acceptors (Kuroyama and Tsumuraya, 2001; Urahara *et al.*, 2004). We therefore measured the incorporation of Xyl from radiolabeled UDP-Xyl by detergent-treated microsomal membranes, derived from the base of stem, in the presence or absence of an exogenous β(1,4)Xyl$_6$ acceptor (Figure 7). The incorporation of label from UDP-Xyl increased considerably when wild-type and *irx3-4* microsomes were incubated with β(1,4)Xyl$_6$. Substantial increases in incorporation were also seen after the addition of β(1,4)Xyl$_6$ to membranes from *irx7*, *irx8* and *parvus-3*, suggesting that these lines have the ability to transfer [^{14}C]Xyl from UDP-[^{14}C]Xyl onto β(1,4)-xylooligosaccharides. In contrast, *irx9* and *irx14* exhibited no apparent stimulation in the incorporation of radiolabel from UDP-Xyl in the presence of exogenous β(1,4)Xyl$_6$.

Discussion

Our previous studies have demonstrated the effectiveness of identifying genes on the basis of co-variance with known secondary cell-wall markers (Brown *et al.*, 2005).

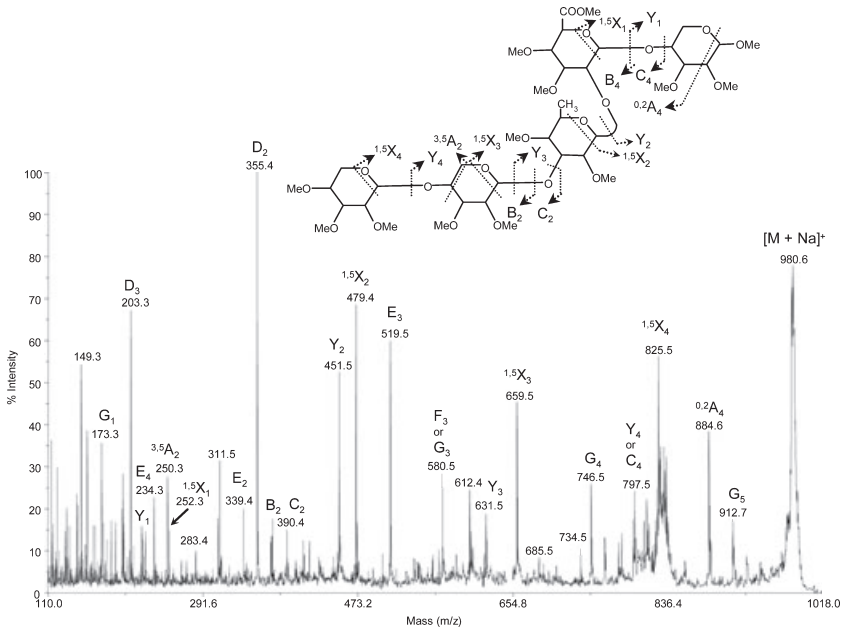

Figure 6. Identification of the structure of the reducing-end oligosaccharide by MALDI-TOF/TOF tandem mass spectrometry.
Oligosaccharides produced by xylanase digestion of wild-type cell-wall xylan were perdeuteromethylated and analysed by MALDI-MS/MS. The series of Y_n and $^{1,5}X_n$ fragment ions (nomenclature according to Domon and Costello, 1988) confirmed the sequence to be pentose–pentose–deoxyhexose–hexuronic acid–pentose. Other ions in the spectrum (e.g. E_n, D_n, G_n) indicate branching and linkage positions.

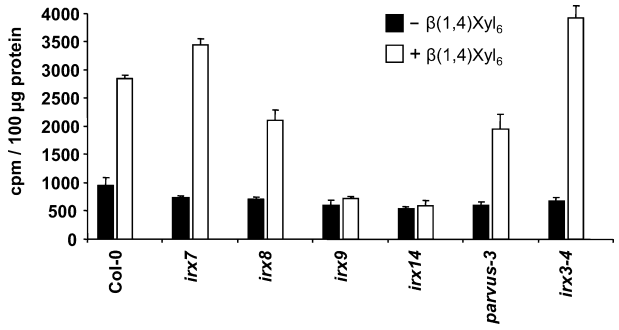

Figure 7. Xylosyltransferase activity catalysed by Arabidopsis microsomal membranes.
Comparison of xylosyltransferase activity in wild-type and mutant lines in the presence or absence of an exogenous acceptor (1 mM β(1,4)Xyl_6). The results shown are from an average of three assays from one set of plants, and are consistent with those of a similar experiment carried out on another set of independently grown plants. Standard error bars for triplicate assays are shown.

The function of the majority of these genes remains unknown, and identifying their role in secondary cell-wall deposition remains a major challenge.

In an initial analysis of genes expressed during secondary cell-wall formation (Brown *et al.*, 2005), three mutants were isolated that exhibited large Xyl deficiencies attributed to a decrease in xylan content. The genes corresponding to these mutants encode putative glycosyltransferases. Using these same methods, with the addition of more publicly available microarray data, two additional genes encoding putative glycosyltransferases have now been identified. Analyses of the corresponding insertion mutants, *irx14* and *parvus-3*, identified a number of characteristics in common with *irx7*, *irx8* and *irx9*. Both *irx14* and *parvus-3* gave clear *irx* phenotypes, and decreases in Xyl in the inflorescence stem that were comparable in severity to those in *irx7*, *irx8* and *irx9* (Figures 1, 3 and 4). All five show a similar decrease in xylan quantity measured by PACE, similar trends in changes to the cell-wall FTIR spectrum, and a similar increase in the proportion of xylan branching by Me-GlcUA relative to GlcUA (Figures 2, 4 and 5).

Several lines of evidence point to these mutants being defective specifically in xylan synthesis. These xylan synthesis defects lead to secondary alterations in other wall polysaccharides. Previous work had suggested a potential role for PARVUS in the synthesis of pectin. Lao *et al.* (2003) demonstrated that the *parvus* mutant had differences in the ratio of 2- to 2,4-linked Rhamnose (Rha) in leaf cell walls compared with wild-type, which the authors ascribed to a change in RGI branching. However, a reduction was also observed in β(1-4)-linked Xyl residues. Changes in pectic epitopes have been observed in several severely dwarfed secondary cell-wall mutants. *mur10*, allelic to *irx3*, exhibits an increase in α(1-5)-Arabinan epitopes in the hypocotyl (Bosca *et al.*, 2006), whilst *irx8* exhibits reductions in GalUA associated with homogalacturonan in pectinase-released cell-wall fractions (Persson *et al.*, 2007). In *irx8*, these changes have been attributed to a reduction in the interactions between xylan and pectic polymers (Persson *et al.*, 2007). The four other xylan-deficient mutants described in this study also exhibited alteration in the composition of pectic cell-wall fractions. However, these alterations are relatively minor, and are dwarfed by the decrease in xylan in the cell-wall hemicellulose fractions.

The cellulose content of both *irx14* and *parvus-3* increased during stem development in a manner similar to that in wild-type, reflecting the increased cellulose deposition during

secondary cell-wall formation. In common with *irx7*, *irx8* and *irx9* (Brown *et al.*, 2005), however, the cellulose content of the stem was less than in the corresponding wild-type plants (Figure 2b). We believe this decrease in cellulose results directly or indirectly from the xylan synthesis defect, through the alteration in plant morphology. The reduction in xylan synthesis is unlikely to be due to a cellulose synthesis deficiency, as severe cellulose-deficient mutants such as *irx3-4* apparently exhibit an increase in xylan biosynthesis (Figures 3 and 5). Indeed, no previously described mutant with decreased cellulose synthesis in the secondary cell wall exhibits a decrease in xylan accumulation (Brown *et al.*, 2005; Turner and Somerville, 1997). Similarly, *irx4*, which is defective in a cinnamoyl CoA reductase gene required for lignin biosynthesis, exhibits a collapsed xylem and altered gross plant morphology but normal levels of xylan (Jones *et al.*, 2001). Together, the results suggest *irx14* and *parvus-3* are likely to be defective in the same metabolic pathway as *irx7*, *irx8* and *irx9*. The cell-wall composition, FTIR, polysaccharide fractionation and PACE analyses presented here corroborate previous studies, and demonstrate that *irx7*, *irx8* and *irx9* are xylan-deficient mutants. Furthermore, *irx14* and *parvus-3* exhibit similar large decreases in xylan consistent with the primary defect in all five mutants being reduced xylan biosynthesis.

The combination of PACE and MALDI-TOF MS analyses has provided a detailed description of xylan branching in Arabidopsis. In wild-type plants, a side branch is added on average to one in eight Xyl residues, with the ratio of Me-GlcUA to GlcUA close to 2 (Figures 4b and 5). In the five xylan-deficient mutants, the GlcUA side chains are decreased to trace amounts. In spite of this, the frequency of side chain branching was similar in all the xylan-deficient mutants, with GlcUA being replaced with Me-GlcUA (Figures 4b and 5). These data clearly demonstrate that a mechanism maintains a similar degree of Xyl substitution whatever the rate of Xyl backbone synthesis. This could occur if synthesis of the backbone and side chains are closely linked as previous studies have suggested (Baydoun *et al.*, 1989). The regulation of branching is apparently independent of the relative proportion of GlcUA to Me-GlcUA substitution of the xylan. It is unclear how the Me-GlcUA side chain on xylan is formed, and whether the methylation occurs at the sugar nucleotide level or once the sugar is attached to the xylan backbone. If the rate of the sugar nucleotide methylation reaction is what regulates the ratio of GlcUA to Me-GlcUA, then low concentrations of UDP-GlcUA could result in it all being converted to the methylated form. Such low concentrations of UDP-GlcUA could arise through perturbations of sugar nucleotide pools as a consequence of impaired UDP-Xyl usage. Indeed, synthesis of UDP-GlcUA is inhibited by UDP-Xyl (Hinterberg *et al.*, 2002; Stewart and Copeland, 1998; Turner and Botha, 2002). Whether this occurs in xylan-deficient mutants remains unclear, and needs to be substantiated by measurements of nucleotide sugar pools. Alternatively, if methylation of GlcUA occurs once it has been transferred to the xylan backbone, as has been suggested (Kauss and Hassid, 1967), it is possible that the lower amount of GlcUA side chain resulting from reduced xylan synthesis would result in all the GlcUA being methylated (Peña *et al.*, 2007).

While all five mutants described in this study exhibit a decrease in xylan, MALDI-TOF MS of the xylan reducing-end oligosaccharide and measurement of enzyme activity separated them into two distinct groups, with *irx9* and *irx14* comprising one group and *irx7*, *irx8* and *parvus* the other. If each unique linkage in xylan is catalysed by a dedicated glycosyltransferase, a minimum of only two or three would be required for xylan chain elongation and side branch addition. However, the oligosaccharide at the reducing ends of Arabidopsis xylan probably requires the action of several additional enzymes for its synthesis. The absence of this oligosaccharide in xylan derived from *irx7* and *irx8* suggests that the enzymes corresponding to these mutants (IRX7 and IRX8) are responsible for its synthesis (Figure S3) (Peña *et al.*, 2007). The oligosaccharide may function as a primer for synthesis, and its absence would lead to impaired xylan chain initiation (Peña *et al.*, 2007). PARVUS may also be required for primer synthesis as the complex oligosaccharide was also absent from xylan extracted from *parvus-3* (Figure 5). This conclusion is further supported by measurements of xylosyltransferase activity in these mutants. Microsomal membranes isolated from wild-type and *irx3-4*, in addition to *irx7*, *irx8* and *parvus-3*, showed a clear increase in xylosyltransferase activity on addition of a $\beta(1,4)Xyl_6$ acceptor, indicating that the capacity to transfer Xyl from UDP-Xyl onto higher $\beta(1,4)$-xylooligosaccharides is not substantially impaired in these mutants. IRX8 and PARVUS belong to a subgroup of GT family 8 proteins named the GAUT1-related super-family of retaining GTs (Sterling *et al.*, 2006). These may catalyse the formation of α-glycosidic bonds using α-linked donor substrates. IRX8 is related to GAUT1, a homogalacturonan galacturonosyltransferase, leading to the suggestion that it catalyses addition of the α-linked GalUA residue to the reducing Xyl residue of the short oligosaccharide sequence (Peña *et al.*, 2007). PARVUS, a member of the GalUAT-like (GATL) family, has also been proposed to function as a putative GalUA transferase on the basis of homology to the GUAT1-related family (Sterling *et al.*, 2006). PARVUS, like IRX8, is therefore also a candidate for catalysis of addition of the α-linked GalUA residue to the reducing Xyl residue. IRX7 is a member of the GT47 family of enzymes with inverting GT activity. As a result it has been proposed that IRX7 could catalyse the formation of one of several β-linkages of Xyl, using α-linked UDP-Xyl, or catalyse the addition of α-linked Rha using β-linked UDP-Rha (Peña *et al.*, 2007). Characterization of the xylan remaining in these mutants is currently underway, and

this may give a more precise prediction on the function of these genes.

IRX9 and IRX14 are members of the GT43 family. To date, this family is known to contain only enzymes with inverting activity. Analysis of *irx9* indicated the presence of the short oligosaccharide sequence at the reducing end of the xylan chain (Figure S3) (Peña *et al.*, 2007). Additional studies have also revealed that the xylan chain length was significantly reduced, leading to a proposal that IRX9 is required for xylan chain elongation (Peña *et al.*, 2007). The data presented in this study suggests that IRX14 is also a candidate for this role. The xylosyltransferase assay supports this theory, as, in contrast to *irx7*, *irx8* and *parvus-3*, incorporation of label from UDP-Xyl was not stimulated by addition of acceptor to membranes of *irx9* or *irx14* (Figure 7). This suggests that both these mutants have an impaired inability to transfer Xyl from UDP-Xyl onto higher β(1,4)-xylooligosaccharides. Also consistent with this view is the observation that, like xylan from *irx9*, the putative oligosaccharide primer is present in xylan from *irx14* (Figure 5). Whether the mechanisms of action of IRX9 and IRX14 are the same remains unclear; however, the identification of two xylan-deficient mutants with reduced xylosyltransferase activity suggests the possibility that an enzyme complex of these two proteins synthesizes xylan. The two GT43 members, IRX9 and IRX14, may be part of a complex that is unstable or non-functional if one of the components is missing. This situation would be similar to the cellulose synthase complex that is required for the formation of β(1-4)-glucose chains (Taylor *et al.*, 2003).

In summary, we describe two novel Xyl-deficient mutants and compare them to three that have been previously described (Bauer *et al.*, 2006; Brown *et al.*, 2005; Peña *et al.*, 2007; Persson *et al.*, 2007; Zhong *et al.*, 2005). Detailed biochemical characterization of the cell walls from these mutants indicates that they are all xylan-deficient. By comparing the mutants, we found that the frequency of side branching of xylan remains essentially constant despite large reductions in GlcUA side branches. We were able to classify the mutants based on reducing-end oligosaccharide structure and enzyme activity. It would be hard to derive similar conclusions on possible enzyme function from the analysis of mutants individually, and therefore the work demonstrates the power of analysing several cell-wall mutants simultaneously. Consequently, this study has contributed to our understanding of xylan biosynthesis, and also has general implications for the functional analysis of cell-wall biosynthesis genes.

Experimental procedures

Plant material

Plants were germinated and grown on 0.8% w/v agar plates containing MS nutrients and B5 vitamins (Gamborg *et al.*, 1968; Murashige and Skoog, 1962) for 2 weeks prior to being transferred to compost containing vermiculite and perlite (10:1:1). Plants were then grown at 22°C in controlled-environment cabinets (CLF Plant Climatics; http://www.plantclimatics.de) under a 16 h day light regime of 150–180 μmol m^{-2} sec^{-1}.

Screening of homozygous plants with T-DNA insertions

Identification of homozygous plants with T-DNA insertions in At1g19300 (*parvus-3*, salk_045368) and At4g36890 (*irx14*, salk_038212) was performed as described by Brown *et al.* (2005). Briefly, T-DNA insertions were identified using the flanking primers (LP and RP) generated by the SIGnal T-DNA verification primer design web site (http://signal.salk.edu/tdnaprimers.html) and primers from the T-DNA left border LBa1 (5′-GCGTGGACCGCT-TGCTGCAACT-3′) and LBb1 (5′-TCAAACAGGATTTTCGCCTGCT-3′).

Real-time PCR of plants with T-DNA insertions

Material for RNA analysis was ground in liquid nitrogen, and RNA was isolated using the Qigen RNeasy kit (http://www.qiagen.com/) according to the manufacturer's instructions. T-DNA insertion lines were confirmed as lacking specific mRNA transcript using gene-specific primers. First-strand synthesis was performed on 10 μg of total RNA using 100 U of reverse transcriptase (Promega, http://www.promega.com/) at 42°C for 1 h. The amplification conditions used were as follows: 95°C for 5 min, various number of cycles of 95°C for 15 sec, 60°C for 30 sec and 72°C for 1 min, then 4°C hold using the following primers: At1g19300, LP 5′-CCACTTCGTCGC CTCTGCTT-3′, RP 5′-TTTCCGATGGGCGAAGGTTA-3′; At4g36890, LP 5′-ATGCGGAAGAGATGGTTTTG-3′, RP 5′-TTCGGATTTTCGTTGG-ATGT-3′. Control PCR was performed using 18S-specific primers.

Mutant analysis

Stem sections, approximately 200-μm thick, were hand cut using a razorblade and stained with toluidine blue O (Sigma, http://www.sigmaaldrich.com/) as previously described (Turner and Somerville, 1997). Between 5 and 10 plants were examined for each mutant line. They were viewed on a Leica DMR light microscope (Leica Microsystems; http://www.leica-microsystems.com) and photographed using a Spot RT digital camera (Diagnostic Instruments; http://www.diaginc.com). Analysis of neutral monosaccharides in the non-cellulose fraction of tissue derived from the inflorescence stem was performed using gas chromatography of alditol acetates as described previously (Reiter *et al.*, 1993). Measurements were taken from a pool of 5–7 stems from plants that had 11–13 expanded siliques. Cellulose measurements were performed from individual plants using 5 cm segments from the base of the primary inflorescence stem as previously described (Turner and Somerville, 1997). Three developmental stages were examined: early (plants with 1–3 expanded siliques), middle (plants with 5–7 expanded siliques) and late (plants with 11–13 expanded siliques). FTIR analysis was performed as described by Brown *et al.* (2005) with slight modifications. Four replicates of pooled stem material (5–8 plants) were freeze-dried for 2 days and milled by rapid shaking with a ball-bearing for 30 min using a Tissuelyser (Qiagen) prior to analysis. An Equinox 55 FT-IR spectrometer (Bruker; http://www.bruker.com), fitted with an HTS-XT high-throughput microplate sampling accessory, was used to collect spectra over the wavenumber range of 4000 to 600 cm^{-1}. Only the absorbancies between 2000 and 800 cm^{-1} were used during PC analysis.

Complementation of irx14

The vector for expression of a STREP-tagged *IRX14* construct was constructed using Gateway technology (Invitrogen, http://www.invitrogen.com/) as described by the manufacturer. The destination vector (3HSC) was constructed by inserting the STREP II sequence into the *Xba*I–*Sma*I sites of pUC19, subsequently digesting with *Sma*I, and then ligating with the 'frame A' (Invitrogen) DNA fragment. The resulting product was excised and inserted into pBSK containing a 1.7 kb fragment of the *IRX3* promoter region. The entire insert, excised with *Xho*I and *Sac*I, was ligated into the vector pCB1300 upstream of the NOS terminator sequence. The entry clones were obtained by PCR amplifying a cDNA fragment containing the full-length *IRX14* gene, using the primers S-IRX14F (5′-AAAAAGCAGGCTCGAAGAAGATGAAGCTCTCTGC-3′) and S-IRX14R (5′-AGAAAGCTGGGTATCTGGAGGAGAAGATGATC-3′), and BP clonase II cloning (Invitrogen) into pDONOR. STREP-tagged *IRX14* expression clones were obtained after LR clonase II cloning (Invitrogen) of the entry vector into the 3HSC destination vector The construct was transformed into *irx14* using *Agrobacterium* vacuum infiltration (Clough and Bent, 1998). Transgenic plants were identified by growing on MS medium containing hygromycin.

Cell-wall fractionation

Cell-wall fractionation was based upon the methods described by Coimbra *et al.* (1996) with minor alterations. Freeze-dried and tissue-lysed stem material (approximately 1 g) was immersed in two changes of 70% v/v ethanol at 70°C for 1 h each, washed with acetone and then air-dried overnight. The material was then suspended in chloroform:methanol (1:1) for 1 h at room temperature, filtered onto filter paper (Whatman; http://www.whatman.com), washed with acetone and then air dried. This material was termed alcohol-insoluble material (AIR). AIR (200 mg) was suspended in 10 ml of 0.05 M CDTA (pH 6.5) for 24 h at room temperature. The suspension was centrifuged (48 000 ***g***), and the pellet washed once with distilled H_2O. The supernatants were combined as the CDTA-soluble fraction. The AIR was subsequently extracted under oxygen-free conditions using 0.05 M Na_2CO_3 containing 0.01 M $NaBH_4$ for 24 h at 4°C (Na_2CO_3-soluble fraction), 1 M KOH containing 0.01 M $NaBH_4$ for 24 h at room temperature (1 M KOH-soluble fraction) and then 4 M KOH containing 0.01 M $NaBH_4$ for 24 h at room temperature (4 M KOH-soluble fraction). All fractions were filtered through a GF/C glass fibre filter (Whatman). The Na_2CO_3 and KOH fractions were also chilled on ice and adjusted to pH 5 with glacial acetic acid. All cell-wall fractions were then dialysed extensively against deionized water for 5 days, and then lyophilized. The fractionation was repeated three times on three sets of plants grown independently, and the mean of these three independent replicas was calculated.

Analysis of cell-wall fractions by TMS ethers of methyl glycosides

Analysis of the TMS ethers of methyl glycosides of the cell-wall fractions was performed as previously described (York *et al.*, 1985). Briefly, approximately 5 mg of cell-wall material was incubated in 1 M HCl in methanol for 16 h at 80°C. The methanolic HCl was removed by adding 100 μl butanol and evaporating to dryness using a rotary evaporator. The subsequent methyl glycosides and methyl ester methyl glycosides were then silylated using Sylon (Sigma-Aldrich) for 20 min at 80°C, and evaporated to dryness. The derivates were then dissolved in hexane (1 ml), insoluble salts were removed by centrifugation (30 000 ***g***), and the supernatant evaporated. The residue was dissolved in 100 μl of hexane, of which 1 μl was analysed by GC.

Derivatized samples were analysed using an Agilent 6895 gas chromatograph (Agilent; http://www.agilent.com). Silylated sample (1 μl) was injected via the split injector (split ratio 10:1) into a HP1 column (Agilent) under the following temperature program: an initial temperature of 140°C, then an immediate increase to 180°C at a rate of 2°C/min. Chromatogram peaks were identified on the basis of retention times of arabinose, xylose, galactose, glucose, mannose, rhamnose, glucuronic acid and galacturonic acid sugars. Chromatogram peaks generated by 4-*O*-methyl glucuronic acid were assigned on the basis of retention times of 4-*O*-methyl-α-glucuronic acid (a generous gift from Miroslav Koos, Slovak Academy of Sciences, Bratislava, Slovakia) and by comparing with chromatographs of purified 4-*O*-methyl-glucurono-D-xylan (Sigma-Aldrich).

PACE materials

Endo-β-1,4-xylanase (Xyl10A, glycosylhydrolase family 10) from *Cellvibrio japonicus* was a generous gift from Harry Gilbert (University of Newcastle, UK). Its specificity for β-1,4-xylan was tested using PACE according to the method described by Goubet *et al.* (2002). ANTS (8-aminonaphthalene-1,3,6-trisulfonic acid) and galactose were purchased from Molecular Probes (http://probes.invitrogen.com) and Sigma, respectively. $(Man)_2$ and $(Man)_3$ were purchased from Megazyme (http://www.megazyme.com). Polyacrylamide containing a 29:1 ratio of acrylamide to *N*,*N*′-methylenebisacrylamide was obtained from Severn Biotech (http://www.severnbiotech.com).

Preparation of cell walls for PACE

Stem fractions were incubated for 30 min in 95% ethanol at 65°C to inactivate enzymes, and then were ground in a Mixer Mill MM200 (Glen Creston, Stanmore, Middlesex, UK). The homogenate was centrifuged at 4000 ***g*** for 15 min. The pellet was washed as described by Goubet *et al.* (2002).

Xylan fingerprinting by PACE

Dried cell-wall material (50 μg) was treated with 4 M NaOH (20 μl) for 1 h at room temperature before adjusting to pH 5-6 with HCl (1 M). The hydrolysis was performed in 0.1 M ammonium acetate, pH 6, with 20 mU of Xyl10A overnight. The reactions were stopped by boiling for 30 min, and the samples were dried using a centrifugal vacuum evaporator.

Derivatization of the sugars with ANTS was performed as described previously (Goubet *et al.*, 2002) with samples dissolved in 10 μl of buffer (DMSO:water:acetic acid, 20:17:3). The derivatized sugars were resuspended in 100 μl of 3 M urea and stored before use at −20°C. Separation of ANTS-derivatized sugars, using 1 μl of sample per gel lane, was performed as described by Goubet *et al.* (2002). Control experiments without substrates or enzymes were performed under the same conditions to identify any non-specific compounds in the enzymes, polysaccharides/cell walls or labelling reagents. Gels were scanned and quantified as described previously (Goubet *et al.*, 2002). Standards for quantification [galactose, $(Man)_2$ and $(Man)_3$] were separated alongside samples in each gel to obtain a standard curve of pmol quantity of fluorophore-labelled oligosaccharide. The quantity of Xyl, $(Xyl)_2$ and $GlcUA(Xyl)_3$/

Me-GlcUA(Xyl)$_3$ in 1 μl of sample was calculated using this standard curve. The ratio of Xyl to Glc/Me-Glc was calculated by summing the relative contribution of the Xyl-containing bands = (Xyl)$_1$ x 1 + (Xyl)$_2$ x 2 + ([Me]GlcUA (Xyl)$_3$) x 3, compared to GlcUA/MeGlcUA = ([Me]GlcUA(Xyl)$_3$) x 1.

Xylan fingerprinting by MS

Cell-wall material (500 μg) was treated with 4 M NaOH (50 μl) for 1 h at room temperature before adjustment to pH 5-6 with HCl (1 M). Where indicated, ends were reduced by incubation with $NaBH_4$ (10 mg/ml) for 2 h at room temperature in 0.5 M NaOH, and then adjusted to pH 5.5 with glacial acetic acid. The hydrolysis was performed in 0.1 M ammonium acetate, pH 6, with 100 mU of Xyl10A overnight. The reactions were stopped by boiling for 30 min. The samples were filtered using a Nanosep system (molecular weight cut-off of 10 kDa; Pall; http://www.pall.com) and dried using a centrifugal vacuum evaporator. The resulting oligosaccharides were purified using HyperSep Hypercarb cartridges (Thermo-Hypersil-Keystone; http://www.thermo.com) and subsequently analysed by MALDI-TOF MS. Due to the presence of contaminant signals complicating these native spectra, the remainder of each sample was perdeuteromethylated (using the NaOH slurry method described by Dell *et al.*, 1989) prior to re-analysis by MALDI-TOF MS. All mass spectra were recorded in positive ion mode on a 4700 Proteomics Analyzer(AppliedBiosystems,http://www.appliedbiosystems.com/). This MALDI tandem mass spectrometer uses a 200 Hz frequency triple Nd-YAG laser operating at a wavelength of 355 nm. 2,5-dihydroxybenzoic acid (DHB) (Fluka; http://www.sigmaaldrich.com), dissolved in 50% aqueous methanol, was used as the matrix, and averages of 2500 shots were used to obtain all MS spectra. The MALDI-TOF/TOF tandem mass spectrum for the reducing-end oligosaccharide was acquired manually with an average of 10 000 laser shots. The collision energy was set at 1 kV, and the oligosaccharide ion was collided in the CID cell with argon at a pressure of 2×10^{-6} Torr.

Microsomal membrane isolation

Microsomal membranes were prepared from the inflorescence stems of 6-week-old plants, according to the method described by Porchia and Scheller (2000), with slight modifications. All procedures were carried at 0–4°C. Harvested stems (6 g FW) were ground in a mortar and pestle containing 20 ml 50 mM HEPES-KOH, pH 7.2, 1 mM DTT, 1 mM $MgCl_2$, 5 mM EDTA, 100 mM sodium ascorbate, 0.4 M sucrose, proteinase inhibitor cocktail (Complete tablets, EDTA-free, Roche Applied Science; http://www.roche.com) and 1% w/v polyvinylpolypyrrolidone. The suspension was filtered through a 50 μm nylon cloth mesh, and centrifuged at 2500 ***g*** for 15 min. Microsomal membranes were collected by centrifuging the supernatant at 200 000 ***g*** for 1 h, and re-suspending in 180 μl of homogenization buffer without polyvinyl polypyrrolidone.

Xylosyltransferase assay

The xylosyltransferase assays were performed using 300 μg of microsomal membrane protein concentrate determined by Bradford's reagent (Bradford, 1976), and incubated in a total of 40 μl buffer containing 50 mM HEPES-KOH, pH 7, 5 mM $MgCl_2$, 10 mM NaF, 1 mM DTT and UDP-[^{14}C]-D-Xyl (3.7 μM, 1.5 kBq, Perkin Elmer; http://www.perkinelmer.com) with or without 1 mM of the exogenous acceptor β(1,4)Xyl$_6$ (Megazyme; http://www.megazyme.com). The reaction was performed at room temperature (20–24°C) for 30 min, and was then terminated by adding 250 μl of 50% w/v Dowex-1x8 slurry (Sigma). The reaction mixture was then eluted by centrifugation for 2 min at 2000 ***g***. Total radioactivity was determined by adding 2 ml of Ecoscint A liquid scintillation cocktail (National Diagnostics; http://www.nationaldiagnostics.com) and counting by liquid scintillation counter. The assay was repeated three times each on two sets of independently grown plants.

Acknowledgements

We are grateful to Miroslav Koos (University of Bratislava) for supplying 4-*O*-methyl glucuronic acid, Harry Gilbert (Newcastle University) for the xylanase, Aaron Liepman (Eastern Michigan University) for developing the xylosyltransferase assay, and J. William Allwood for help in preparing the FTIR samples. We thank Zhinong Zhang for helping with PACE. Work carried out by D.B. in Manchester and F.G. and E.S. in Cambridge was funded by grants from the Biotechnology and Biological Sciences Research Council (BBSRC) (reference BB/C505632/1 and 8/D19624 respectively). V.W.W. was supported by a studentship from the BBSRC.

Supplementary Material

The following supplementary material is available for this article online:

Figure S1. Expression analysis and complementation of *irx14* and *parvus-3*.

Figure S2. Specific oligosaccharide bands in xylan analysis by PACE.

Figure S3. MALDI-TOF MS spectra showing signals for the perdeuteromethylated [Me]-GlcUA(Xyl)$_3$ oligosaccharides produced by xylanase digestion of cell-wall xylan.

Figure S4. MALDI-TOF MS spectra showing that the complex oligosaccharide is derived from the reducing end of the polysaccharide.

This material is available as part of the online article from http://www.blackwell-synergy.com

Please note: Blackwell Publishing are not responsible for the content or functionality of any supplementary materials supplied by the authors. Any queries (other than missing material) should be directed to the corresponding author for the article.

References

Andersson, S.I. and Samuelson, O. (1983) Structure of the reducing end-groups in spruce xylan. *Carbohydr. Res.* **111**, 283–288.

Aspeborg, H., Schrader, J., Coutinho, P.M. *et al.* (2005) Carbohydrate-active enzymes involved in the secondary cell wall biogenesis in hybrid aspen. *Plant Physiol.* **137**, 983–997.

Barton, C.J., Tailford, L.E., Welchman, H., Zhang, Z.N., Gilbert, H.J., Dupree, P. and Goubet, F. (2006) Enzymatic fingerprinting of Arabidopsis pectic polysaccharides using polysaccharide analysis by carbohydrate gel electrophoresis (PACE). *Planta*, **224**, 163–174.

Bauer, S., Vasu, P., Persson, S., Mort, A.J. and Somerville, C.R. (2006) Development and application of a suite of polysaccharide-degrading enzymes for analyzing plant cell walls. *Proc. Natl Acad. Sci. U.S.A.* **103**, 11417–11422.

Baydoun, E.A.H., Waldron, K.W. and Brett, C.T. (1989) The interaction of xylosyltransferase and glucuronyltransferase involved in glucuronoxylan synthesis in pea (*Pisum sativum*) epicotyls. *Biochem. J.* **257**, 853–858.

Bevan, M.W. and Franssen, M.C.R. (2006) Investing in green and white biotech. *Nature Biotechnol.* **24**, 765–767.

Bosca, S., Barton, C.J., Taylor, N.J., Ryden, P., Neumetzler, L., Pauly, M., Roberts, K. and Seifert, G.J. (2006) Interactions between mur10/cesA7 dependent secondary cellulose biosynthesis and primary cell wall structure. *Plant Physiol.* **142**, 1353–1363.

Bradford, M.M. (1976) Rapid and sensitive method for quantitation of microgram quantities of protein utilizing the principle of protein–dye binding. *Anal. Biochem.* **72**, 248–254.

Brown, D.M., Zeef, L.A.H., Ellis, J., Goodacre, R. and Turner, S.R. (2005) Identification of novel genes in Arabidopsis involved in secondary cell wall formation using expression profiling and reverse genetics. *Plant Cell*, **17**, 2281–2295.

Clough, S.J. and Bent, A.F. (1998) Floral dip: a simplified method for *Agrobacterium*-mediated transformation of *Arabidopsis thaliana*. *Plant J.* **16**, 735–743.

Coimbra, M.A., Delgadillo, I., Waldron, K.W. and Selvendran, R.R. (1996) Isolation and analysis of cell wall polymers from olive pulp. In *Modern Methods of Plant Analysis, volume 17: Plant Cell Wall Analysis* (Linskens, H.F. and Jackson, J.F., eds). Berlin: Springer, pp. 20–43.

Coutinho, P.M. and Henrissat, B. (1999) *Carbohydrate-Active Enzymes: An Integrated Database Approach*. Cambridge: Royal Society of Chemistry.

Coutinho, P.M., Deleury, E., Davies, G.J. and Henrissat, B. (2003) An evolving hierarchical family classification for glycosyltransferases. *J. Mol. Biol.* **328**, 307–317.

Dell, A., Khoo, K.-H., Panico, M., McDowell, R.A., Etienne, A., Reason, A.J., Morris, H.R. (1992) FAB-MS and ESI-MS of glycoproteins. In *Glycobiology. A Practical Approach* (Fukuda, M., Kobata, A., eds). Oxford, Oxford University Press, vol. 125, pp. 187–222.

Domon, B. and Costello, C.E. (1988) A systematic nomenclature for carbohydrate fragmentations in FAB-MS/MS spectra of glycoconjugates. *Glycoconjugate J.* **5**, 397–409.

Ebringerova, A. and Heinze, T. (2000) Xylan and xylan derivatives – biopolymers with valuable properties. Naturally occurring xylan structures, procedures and properties. *Macromol. Rapid Commun.* **21**, 542–556.

Fry, S.C. (2000) *The Growing Plant Cell Wall: Chemical And Metabolic Analysis*. Caldwell, NJ: The Blackburn Press.

Gamborg, O.L., Miller, R.A. and Ojima, K. (1968) Nutrient requirements of suspension cultures of soybean root cells. *Exp. Cell Res.* **50**, 151–154.

Goubet, F., Jackson, P., Deery, M.J. and Dupree, P. (2002) Polysaccharide analysis using carbohydrate gel electrophoresis: a method to study plant cell wall polysaccharides and polysaccharide hydrolases. *Anal. Biochem.* **300**, 53–68.

Handford, M.G., Baldwin, T.C., Goubet, F., Prime, T.A., Miles, J., Yu, X.L. and Dupree, P. (2003) Localisation and characterisation of cell wall mannan polysaccharides in *Arabidopsis thaliana*. *Planta*, **218**, 27–36.

Hinterberg, B., Klos, C. and Tenhaken, R. (2002) Recombinant UDP-glucose dehydrogenase from soybean. *Plant Physiol. Biochem.* **40**, 1011–1017.

Johansson, M.H. and Samuelson, O. (1977) Reducing end groups in birch xylan and their alkaline degradation. *Wood Sci. Technol.* **11**, 251–263.

Jones, L., Ennos, A.R. and Turner, S.R. (2001) Cloning and characterization of *irregular xylem4* (*irx4*): a severely lignin-deficient mutant of Arabidopsis. *Plant J.* **26**, 205–216.

Kauss, H. and Hassid, W.Z. (1967) Biosynthesis of 4-*O*-methyl-D-glucuronic acid unit of hemicellulose b by transmethylation from *S*-adenosyl-L-methionine. *J. Biol. Chem.* **242**, 1680–1684.

Kuroyama, H. and Tsumuraya, Y. (2001) A xylosyltransferase that synthesizes β-(1-4)-xylans in wheat (*Triticum aestivum* L.) seedlings. *Planta*, **213**, 231–240.

Lao, N.T., Long, D., Kiang, S., Coupland, G., Shoue, D.A., Carpita, N.C. and Kavanagh, T.A. (2003) Mutation of a family 8 glycosyltransferase gene alters cell wall carbohydrate composition and causes a humidity-sensitive semi-sterile dwarf phenotype in Arabidopsis. *Plant Mol. Biol.* **53**, 687–701.

Maslen, S.L., Goubet, F., Adam, A., Dupree, P. and Stephens, E. (2007) Structure elucidation of arabinoxylan isomers by normal phase HPLC-MALDI-TOF/TOF-MS/MS. *Carbohydr. Res.* **342**, 724–735.

Murashige, T. and Skoog, F. (1962) A revised medium for rapid growth and bioassays with tobacco tissue cultures. *Physiol. Plant.* **15**, 473–480.

Peña, M.J., Zhong, R., Zhou, G.-K., Richardson, E.A., O'Neill, M.A., Darvill, A.G., York, W.S. and Ye, Z.-H. (2007) Arabidopsis *irregular xylem8* and *irregular xylem9*: implications for the complexity of glucuronoxylan biosynthesis. *Plant Cell*, **19**, 549–563.

Persson, S., Wei, H.R., Milne, J., Page, G.P. and Somerville, C.R. (2005) Identification of genes required for cellulose synthesis by regression analysis of public microarray data sets. *Proc. Natl Acad. Sci. U.S.A.* **102**, 8633–8638.

Persson, S., Caffall, K.H., Freshour, G., Hilley, M.T., Bauer, S., Poindexter, P., Hahn, M.G., Mohnen, D. and Somerville, C. (2007) The Arabidopsis *irregular xylem* 8 mutant is deficient in glucuronoxylan and homogalacturonan, which are essential for secondary cell wall integrity. *Plant Cell*, **19**, 237–255.

Porchia, A.C. and Scheller, H.V. (2000) Arabinoxylan biosynthesis: identification and partial characterization of beta-1,4-xylosyltransferase from wheat. *Physiol. Plant.* **110**, 350–356.

Prassinos, C., Ko, J.H. and Han, K.H. (2005) Transcriptome profiling of vertical stem segments provides insights into the genetic regulation of secondary growth in hybrid aspen trees. *Plant Cell Physiol.* **46**, 1213–1225.

Ragauskas, A.J., Williams, C.K., Davison, B.H. *et al.* (2006) The path forward for biofuels and biomaterials. *Science*, **311**, 484–489.

Reiter, W.D., Chapple, C.C.S. and Somerville, C.R. (1993) Altered growth and cell-walls in a fucose-deficient mutant of Arabidopsis. *Science*, **261**, 1032–1035.

Shao, M., Zheng, H., Hu, Y., Lui, D., Jang, J., Ma, H. and Huang, H. (2004) The gaolaozhuangren1 gene encodes a putative glycosyltransferase that is critical for normal development and carbohydrate metabolism. *Plant Cell Physiol.* **45**, 1453–1460.

Spina, E., Sturiale, L., Romeo, D., Impallomeni, G., Garozzo, D., Waidelich, D. and Glueckmann, M. (2004) New fragmentation mechanisms in matrix-assisted laser desorption/ionization time-of-flight/time-of-flight tandem mass spectrometry of carbohydrates. *Rapid Commun. Mass Spectrom.* **18**, 392–398.

Sterling, J.D., Atmodjo, M.A., Inwood, S.E., Kolli, V.S.K., Quigley, H.F., Hahn, M.G. and Mohnen, D. (2006) Functional identification of an Arabidopsis pectin biosynthetic homogalacturonan galacturonosyltransferase. *Proc. Natl Acad. Sci. U.S.A.* **103**, 5236–5241.

Stewart, D.C. and Copeland, L. (1998) Uridine 5′-diphosphate-glucose dehydrogenase from soybean nodules. *Plant Physiol.* **116**, 349–355.

Taylor, N.G., Howells, R.M., Huttly, A.K., Vickers, K. and Turner, S.R. (2003) Interactions among three distinct cesA proteins essential for cellulose synthesis. *Proc. Natl Acad. Sci. U.S.A.* **100**, 1450–1455.

Turner, W. and Botha, F.C. (2002) Purification and kinetic properties of UDP-glucose dehydrogenase from sugarcane. *Arch. Biochem. Biophys.* **407**, 209–216.

Turner, S.R. and Somerville, C.R. (1997) Collapsed xylem phenotype of Arabidopsis identifies mutants deficient in cellulose deposition in the secondary cell wall. *Plant Cell*, **9**, 689–701.

Urahara, T., Tsuchiya, K., Kotake, T., Tohno-oka, T., Komae, K., Kawada, N. and Tsumuraya, Y. (2004) A β-(1,4)-xylosyltransferase involved in the synthesis of arabinoxylans in developing barley endosperms. *Physiol. Plant.* **122**, 169–180.

York, W.S., Darvill, A.G., McNeil, M., Stevenson, T.T. and Albersheim, P. (1985) Isolation and characterization of plant cell walls and cell wall components. *Methods Enzymol.* **18**, 3–40.

Zhong, R.Q., Pena, M.J., Zhou, G.K., Nairn, C.J., Wood-Jones, A., Richardson, E.A., Morrison, W.H., Darvill, A.G., York, W.S. and Ye, Z.H. (2005) Arabidopsis *fragile fiber8*, which encodes a putative glucuronyltransferase, is essential for normal secondary wall synthesis. *Plant Cell*, **17**, 3390–3408.

Zimmermann, P., Hirsch-Hoffmann, M., Hennig, L. and Gruissem, W. (2004) Genevestigator Arabidopsis microarray database and analysis toolbox. *Plant Physiol.* **136**, 2621–2632.

